This is a repository copy of *Microbes influence the biogeochemical and optical properties of maritime Antarctic snow.*.

White Rose Research Online URL for this paper:
https://eprints.whiterose.ac.uk/116847/

Version: Published Version

**Article:**

## RESEARCH ARTICLE

**Key Points:**
- Microbial activity in wet Antarctic snow is detectable from its organic and inorganic carbon contents and the $CO_2$ of interstitial air
- Snow algae cause absorption of visible light and thus more melting due to carotenoid and chlorophyll pigment development
- Inland Antarctic glacial snowpacks have far less diverse microbial communities than coastal snowpacks

**Supporting Information:**
- Supporting Information S1
- Data Set S1

**Correspondence to:**
A. J. Hodson,
a.j.hodson@sheffield.ac.uk

# Microbes influence the biogeochemical and optical properties of maritime Antarctic snow

A. J. Hodson[1,2] (ID), A. Nowak[1] (ID), J. Cook[1] (ID), M. Sabacka[3], E. S. Wharfe[1], D. A. Pearce[4] (ID), P. Convey[5], and G. Vieira[6] (ID)

[1]Department of Geography, University of Sheffield, Sheffield, UK, [2]Arctic Geology, University Centre in Svalbard, Longyearbyen, Norway, [3]School of Geographical Sciences, University of Bristol, Bristol, UK, [4]Faculty of Health and Life Sciences, University of Northumbria, Newcastle upon Tyne, UK, [5]British Antarctic Survey, Cambridge, UK, [6]IGOT, Centre for Geographical Studies, Universidade de Lisboa, Lisbon, Portugal

**Abstract** Snowmelt in the Antarctic Peninsula region has increased significantly in recent decades, leading to greater liquid water availability across a more expansive area. As a consequence, changes in the biological activity within wet Antarctic snow require consideration if we are to better understand terrestrial carbon cycling on Earth's coldest continent. This paper therefore examines the relationship between microbial communities and the chemical and physical environment of wet snow habitats on Livingston Island of the maritime Antarctic. In so doing, we reveal a strong reduction in bacterial diversity and autotrophic biomass within a short (<1 km) distance from the coast. Coastal snowpacks, fertilized by greater amounts of nutrients from rock debris and marine fauna, develop obvious, pigmented snow algal communities that control the absorption of visible light to a far greater extent than with the inland glacial snowpacks. Absorption by carotenoid pigments is most influential at the surface, while chlorophyll is most influential beneath it. The coastal snowpacks also indicate higher concentrations of dissolved inorganic carbon and $CO_2$ in interstitial air, as well as a close relationship between chlorophyll and dissolved organic carbon (DOC). As a consequence, the DOC resource available in coastal snow can support a more diverse bacterial community that includes microorganisms from a range of nearby terrestrial and marine habitats. Therefore, since further expansion of the melt zone will influence glacial snowpacks more than coastal ones, care must be taken when considering the types of communities that may be expected to evolve there.

## 1. Introduction

Snow is the most expansive terrestrial habitat in Antarctica, yet we know almost nothing about the resident ecosystem within it. As a result, we are unable to quantify the consequences that increased melting of Antarctic snow will have for downstream ecosystems. The potential influence of terrestrial snowmelt on coastal ecosystems could be particularly significant. For example, *Dierssen et al.* [2002] identified enhanced marine primary production up to 100 km offshore during high melt years in the Palmer Station area. Presently, melting snow covers up to 20% of the Antarctic surface area during summer and contributes about 350 km$^3$ yr$^{-1}$ or ~83% of all surface and near-surface-derived melt water according to distributed surface energy balance models [*Liston and Winther*, 2005]. However, climate warming has already doubled snowmelt in the Antarctic Peninsula region during the middle part of the 20th century (from 28 Gt a$^{-1}$ to 54 Gt a$^{-1}$ [*Vaughan*, 2006]) and is projected to do so once more over the first half of the 21st century. Two urgent consequences need to be addressed as a result of the increased melting. First, we need to know what proportion of the nutrient resource within snow and ice is at risk from mobilization by meltwater, and second, we need to know the extent to which the resident microbial community within the snow will regulate or transform this nutrient resource as a result of in situ biological production. Since viable microorganisms have been reported in Antarctic snow as far inland as the South Pole [*Carpenter et al.*, 2000], it seems reasonable to expect snowpack microbial processes to potentially influence snow biogeochemistry anywhere on the ice sheet that is subject to melting. For example, using a solute mass balance approach, *Hodson* [2006] showed how 66% of NH$_4^+$ and 74% of PO$_4^{3-}$ in a Signy Island (South Orkney Island Group) snowpack were assimilated in snow, slush, and ice marginal habitats following the onset of melt.

If Antarctic snow represents an important ecosystem in its own right, then addressing uncertainty over the biomass and activity of its resident microorganisms will improve our understanding of melt-driven greenhouse gas exchange across the largest terrestrial interface with Antarctica's atmosphere (i.e., the net

ecosystem exchange of $CO_2$ across the air-snow boundary). So far, the only measurements of photosynthesis in surface and near-surface snows in Antarctica have been conducted upon Signy Island [*Fogg*, 1968]. These have indicated areal rates of up to 10 mgC $m^{-2} d^{-1}$ by snowpacks with up to 5000 cells $mL^{-1}$ of snow algae, but it is not known whether these measurements are representative of other snow covers in Antarctica. Nor is it clear how rates of primary production vary seasonally and are offset by heterotrophic production. Furthermore, these incubations often require handling radioactive chemicals, which is challenging both physically and from a legislative perspective when working in Antarctica. These incubations are also short-lived experiments, and so their contribution to seasonal biological production during the summer needs careful assessment, or at the very least, lots of replication. Much more therefore could be done to understand the seasonal ecology and activity of snowpack ecosystems using alternative methods. One of the purposes of this paper is to help accelerate this research need through the identification of optical and biogeochemical measurements that link quantitatively to ecosystem characteristics such as microbial biomass and productivity.

Developing a quantitative understanding of Antarctic snow ecosystems means we will be well placed to explore the "feedbacks" imposed by changes in snow cover that result from a warmer Antarctica. In addition to the $CO_2$ exchanges and the provision of new or transformed nutrients for downstream marine ecosystems, these feedbacks also include the longevity of the snow cover in areas subject to melting on account of the darkening of the snow by pigments associated with microbial biomass: an effect that is well known from studies outside Antarctica [e.g., *Cook et al.*, 2017; *Kohshima et al.*, 1994; *Thomas and Duval*, 1995]. However, so far, this feedback has been completely neglected in Antarctica, in spite of the frequent occurrence of heavily pigmented snow algal blooms in coastal environments [e.g., *Edwards et al.*, 2004; *Fujii et al.*, 2010].

This paper therefore aims to demonstrate the linkages between key physical, chemical, and biological characteristics in Antarctic snow and assess the extent to which they present a compelling case for an active and important resident microbial ecosystem. In so doing, we provide representative measurements from Livingston Island of the South Shetland group of the maritime Antarctic for future comparison to snowpacks elsewhere in Antarctica and the terrestrial cryosphere. We also demonstrate differences between the optical properties, biogeochemistry, autotrophic biomass, and biodiversity of coastal snowpacks and their inland glacial counterparts using a range of techniques implemented during the 2013/2014 austral summer.

## 2. Materials and Methods

### 2.1. Site Description

Data are presented that describe the chemical, physical, and biological characteristics of five snow sampling sites (hereafter "SP0 to SP4") on the Hurd Peninsula region of Livingston Island during the 2013/2014 field season. The island is within the South Shetland Island group and has a mean annual air temperature of ~ −1°C at the coast [*Bañón et al.*, 2013]. Hurd Peninsula is highly glacierized, and therefore, rudimentary soils are exposed on less than 25% of the land area. Three of the sites (hereafter "coastal snowpacks," called SP0, SP1, and SP2) were located within 100 m of the shoreline. Two others (hereafter "glacial snowpacks" and called SP4 and SP3) were located 500 and 750 m inland respectively (Figure 1). The coastal snowpacks were notable for visible red colored algal snow and, at SP2 only, the presence of green algal snow. No discolouration of surface snows was discernible to the eye at either SP3 or SP4. The underlying substratum differed between the coastal and glacial snowpacks and included glacier ice (SP3 and SP4), beach material (SP0), glacial moraine (SP1), and fluvial outwash plain (SP2). All of the snowpacks were perennial and showed distinct dust horizons that had most likely formed at the end of the preceding 2012/2013 austral summer.

### 2.2. Snow Sampling and Analysis

The work presented here was conducted between days of year (DOYs) 23 and 48, encompassing the transition from peak summer to late summer, which was marked by two significant snowfalls either side of DOY 41. Triplicate samples from the top, middle, and basal snow/ice were collected as part of three surveys conducted on DOYs 23, 35, and 46. In all cases, ~350 g of snow was sampled using a new aluminum snow shovel precleaned with local snow. Samples were stored frozen in sterile 700 mL Whirlpak Bags until processing and preliminary analysis at the Bulgarian St Okhridski Antarctic Station. Powder-free nitrile gloves were worn and used to handle all samples. Sample processing was typically undertaken within a day or so, after letting the samples thaw at room temperature in batches of 12. After thawing, the samples were agitated and a 50 mL
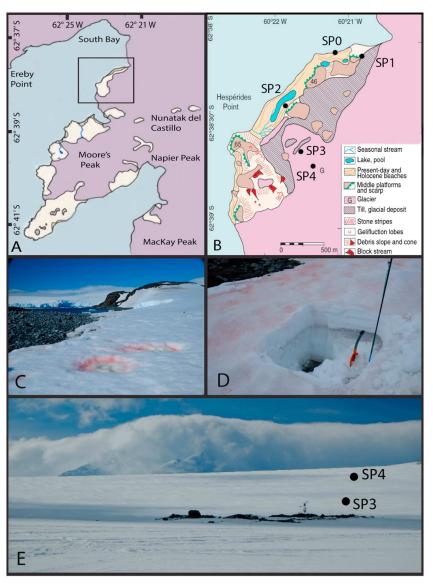
**Figure 1.** (a) Hurd Peninsula of Livingston Island with (b) inset showing geomorphological features of the sampling area [after *López-Martínez et al.*, 2012] and photographs showing (c) SP2, (d) SP0, and (e) SP3 and SP4.

aliquot removed for a fluorescence measurement using a Chelsea Unilux fluorimeter configured for in vivo Chlorophyll *a* detection with a notional detection limit of 0.01 μg L$^{-1}$ and a factory calibration established using diatom cultures. Afterward, we calibrated the Chlorophyll *a* results using samples filtered onto Whatman GFF papers and analyzed using the methanol extraction protocol of *Marker and Jinks* [1982].

Further snowmelt aliquots were analyzed for biogeochemical parameters. First, an unfiltered 50 mL subsample was used for pH and electrical conductivity (EC) determination using a multiparameter Hach Lange HQ 40D with dedicated calibration solutions. A second subsample was then filtered through 0.45 μm Whatman cellulose nitrate filter papers using a prerinsed Nalgene filter holder and hand pump for major ion analysis (see below). A third aliquot was also removed using a sterile syringe and stored in the dark at 4°C within sterile 15 mL Eppendorf tubes after fixing with 3.5% (final concentration) formalin. These samples were intended for flow cytometry analysis in the UK, although a majority were lost by airline baggage handlers in Chile. Finally, during the first and final snow surveys only (i.e., DOYs 23 and 46), a 50 mL aliquot was also filtered through a Whatman GFF filter paper (notional pore space: 0.7 μm) and stored in prerinsed 40 mL glass vials for dissolved organic carbon (DOC) analyses using the membrane conductometric method. This

employed a portable Sievers 5310 Analyzer with UV and persulphate digestion (detection limit 0.01 mg $L^{-1}$ and <5% precision errors according to repeat analysis of midrange (0.4 mg $L^{-1}$) standards). Water samples returned to Sheffield for major ion detection were analyzed using Dionex ICS90 ion chromatography modules, calibrated in the range of 0–2 mg $L^{-1}$. Here we present $Na^+$ and $Cl^-$ as tracers for marine aerosol, nonmarine $Ca^{2+}$ for dust and debris effects, and $NH_4^+$ for nutrient enrichment via penguin guano and seal excreta. Precision errors for these ions were less than 5%, and the detection limit was 0.05 mg $L^{-1}$ for $Cl^-$ and 0.001 mg $L^{-1}$ for $Na^+$, $NH_4^+$, and $Ca^{2+}$. Since the samples could be neither frozen nor preserved during transit, $NH_4^+$ levels are intended to be indicative only.

### 2.3. Microbiological Analysis

A Partec Cyflow flow cytometer was employed to enumerate cells in the 15 mL snow samples fixed with formalin. Quantitative counting of autofluorescent cells with a 488 nm laser recording forward scatter, side scatter, and autofluorescence at standard FL1, FL2, and FL3 wavelengths was employed. FL3 events were therefore used to estimate the number of cells after processing the data using gating rules established from the analysis of blank samples. Blanks were 0.2 μm filtered deionized water and snowmelt, the former being the sheath fluid used for the cytometer. Repeat analyses and enumeration of cells using FL3 indicated a precision error (coefficient of variation) of 4.8% for a sample with an average number of chlorophyll *a*-containing cells of $2.5 \times 10^4$ $mL^{-1}$. An epifluorescence microscope (Zeiss Axioplan 2) was then used to qualitatively assess whether the autofluorescent community was dominated by single-celled snow algae or cyanobacteria.

During the final snow survey of DOY 46, integrated samples of at least 2 kg of snow were collected in large, sterile Whirlpak bags from the top, middle, and basal snow/ice. All samples were handled aseptically from downwind of the sample location using gloves and sterile, bagged equipment. Samples were then double-bagged in a second Whirlpak bag for thawing at room temperature, then syringe filtered immediately through a sterile 0.2 μm Sterivex™ cartridge, before being frozen at −20°C for subsequent 16S rRNA sequencing and sequence analysis. During the latter, negative controls were taken and blanks added to the sequencing reactions. DNA was isolated using MoBio PowerWater® DNA Isolation Kit. The highly variable V3/V4 region of the 16S rRNA was amplified with bacterial primers S-D-Bact-0341-b-S-17 forward and S-D-Bact-0785-a-A-21 reverse, with overhang illumina adaptor attached to the primer sequences, creating a single amplicon of ~460 bp [*Klindworth et al.*, 2013]. The reaction was carried out in 50 μL volumes containing 0.3 mg $mL^{-1}$ bovine serum albumin, 250 μM deoxynucleotide triphosphates, 0.5 μM of each primer, 0.02 U Phusion High-Fidelity DNA Polymerase (Finnzymes OY, Espoo, Finland), and 5× Phusion HF Buffer containing 1.5 mM $MgCl_2$. The following polymerase chain reaction conditions were used: initial denaturation at 95°C for 5 min, followed by 25 cycles consisting of denaturation (95°C for 40 s), annealing (55°C for 2 min) and extension (72°C for 1 min), and a final extension step at 72°C for 7 min. Samples were sequenced using illumina MiSeq platform at Liverpool Centre for Genomics Research and generated 2 × 300 bp overlapping pair-end reads. The 16S sequences were further processed using mothur (v. 1.35) pipeline [*Schloss et al.*, 2009]. Chimeric sequences were identified and removed using UCHIME [*Edgar et al.*, 2011]. Reads were clustered into operational taxonomical units (OTUs), based on at least 97% sequence similarity, and assigned taxonomical identification against SILVA bacterial database [*Quast et al.*, 2013]. The nucleotide sequence data were deposited in GenBank under accession numbers SAMN06368443 to SAMN06368447.

### 2.4. Snow Air Sampling

On three occasions at the beginning of the field campaign (i.e., straight after the first sampling survey on DOYs 26, 27, and 29) and two occasions toward the end of the observation period (DOYs 41 and 48), triplicate 15 mL samples of interstitial air were abstracted from three or more levels in the snowpack at each site using a crevasse probe, 2 mm tubing, and a three-way luer-lock stop cock. The depths of air sample abstraction were 5 cm and then typically every ~50 cm beneath the surface, depending upon the presence of large ice lenses or water at the base of the snow. These cases usually resulted in the deepest snow air samples being collected at depths between 80 and 120 cm. The samples were sealed and analyzed within 1 h of collection using a PP Systems EGM4 Infrared gas analyzer, which used a soda lime scrubber for auto-zeroing every 2 min. Since a $CO_2$ standard was not available, ambient air samples were used as references when the power generator for the local research station had been switched off (every afternoon). These were

sampled upwind of the research station at 1 m above the snow surface. Additional blanks were also run using an ambient air sample that was drawn slowly through a 60 mL syringe filled with soda lime.

### 2.5. Transect Study at SP2

The SP2 site was a distinct, persistent "blizzard tail" accumulation of snow of up to ~4 m depth in a gentle, 30 m long slope that descended toward the shore. The site offered a range of both red and green colored algal blooms with variable cell densities, allowing the impact of biomass upon the spectral reflectance properties of the snow surface to be studied. The red colored snow algae were distributed in a patchy, heterogeneous manner and found anywhere on the slope. However, the green algae were all found near the coastal margin of the snow slope, most often upon the surface of basal ice layers that were being progressively revealed by snowmelt and often inundated with melt water. On DOY 41, a total of 7 green and 11 red colored algal bloom patches (10 cm diameter disks) were chosen before being imaged with a digital camera next to a spectralon white reference plate. The surface reflectance of each disk was then measured 10 times and averaged. Each time, the reference plate was sampled in the same manner. All measurements were collected normal to the snow surface using a Stellar Net Bluewave spectrometer and fiber optic with a collimating lens whose field of view enabled ~50% of the surface area of the disk to be sampled at any one time. The conditions were 100% overcast, and the measurements were taken 2 h after solar noon when irradiance was dominated by diffuse light. Measurements were made within the spectral range of 380–900 nm with a resolution of 0.5 nm, thereby capturing most of the visible and near-infrared wave band where most incident solar energy is concentrated and where ice and snow are by far the most reflective. After the reflectance and camera imaging, a disk of snow was sampled to a depth of 2 cm and melted immediately at room temperature for in vivo Chlorophyll *a* measurement by fluorescence and then filtration onto GFF for Chlorophyll *a* analysis by extraction (see above). A subsample of the snow was retained for analysis by flow cytometry, also in the manner described above.

### 2.6. Spectral Profiling of Snow

In addition to the surface reflectance work described above, the spectrometer and a fiber optic were used to measure the spectral characteristics of upwelling light at each of the five snowpit sites. Therefore, a narrow crevasse probe was progressively inserted into the snow prior to the insertion of the fiber optic and the collection of five averaged spectra. Measurements were taken at 5 cm intervals near the surface and down to 50 cm depth. Thereafter, measurements were either taken ~5 cm above the base of the snowpit, or at 40–50 cm intervals (often complicated by the presence of ice lenses). Depth profiles of the upwelling spectra were collected on DOYs 29 and 41 in order to characterize the propagation of light at the start and end of the field campaign.

## 3. Results

Meteorological conditions during the field campaign were not constant and included two periods of snowfall, followed by significant snowdrift redistribution. Therefore, by DOY 41, there was 15 and 29 cm of fresh snow deposited upon the older surface at SP4 and SP3, respectively. Continuing to lower elevations, the corresponding amounts were 32, 47, and 51 cm at SP2, SP1, and SP0, respectively. This additional snow was initially a fine-grained, wind-packed layer, although by the end of field campaign (DOY 48) it had undergone metamorphosis into a coarse grained layer that was entirely at the melting point. Therefore, while the initial stages of the field campaign appeared to be characterized by a stable, melting snow surface that had experienced prolonged snow grain metamorphosis, the latter stages were dominated by a thick accumulation of young snow that had undergone far less metamorphosis and melting.

### 3.1. Snowpack Biogeochemistry

Table 1 presents summary statistics of the biogeochemical parameters at each of the snowpit sites following the three surveys. These reveal low ionic strength snowpacks (average EC less than 18 $\mu$S cm$^{-1}$ for all but the last survey at SP1 and SP0) with average pH values in the range of 5.2–5.6. The pH data are notable for low standard deviations and for being strongly correlated with both Ca$^{2+}$ and dissolved inorganic carbon (DIC). These correlations are explored using the full data set below. The data in Table 1 also reveal very different, correlated behavior by Na$^+$ and Cl$^-$. Therefore, the dominant ionic constituents of the snowpack formed

**Table 1.** Summary Statistics of the Bulk Snowpit Biogeochemical Parameters During Each of the Three Surveys[a]

| Survey Date | Pit | pH | EC ($\mu$S cm$^{-1}$) | Chll $a$ ($\mu$g L$^{-1}$) | DOC (mg L$^{-1}$) | DIC (mg L$^{-1}$) | Cl (mg L$^{-1}$) | Na (mg L$^{-1}$) | Ca (mg L$^{-1}$) | NH$_4$ (mg L$^{-1}$) |
|---|---|---|---|---|---|---|---|---|---|---|
| DOY 24 | SP4 | 5.40 (0.09) | 5.83 (0.12) | 2.18 (1.25) | 0.24 (0.47) | 0.93 (0.038) | 0.58 (0.21) | 0.40 (0.10) | 0.70 (0.18) | 0.24 (0.02) |
| | SP3 | 5.35 (0.16) | 6.29 (0.74) | 3.92 (0.80) | 0.21 (0.27) | 0.90 (0.038) | 0.54 (0.17) | 0.42 (0.20) | 0.37 (0.07) | 0.02 (0.02) |
| | SP2 | 5.60 (0.55) | 10.62 (3.27) | 41.48 (38.09) | 0.34 (0.19) | 1.24 (0.26) | 1.05 (0.36) | 0.79 (0.31) | 0.96 (0.95) | 0.09 (0.13) |
| | SP1 | 5.68 (0.40) | 12.47 (7.45) | 64.71 (106.5) | 0.37 (0.36) | 1.25 (0.34) | 1.85 (1.08) | 1.06 (0.71) | 1.64 (1.43) | 0.05 (0.02) |
| | SP0 | 5.26 (0.11) | 7.71 (0.90) | 36.92 (45.31) | 0.41 (0.39) | 1.01 (0.18) | 0.83 (0.14) | 0.62 (0.06) | 0.49 (0.19) | 0.06 (0.08) |
| DOY 35 | SP4 | 5.21 (0.19) | 6.18 (1.74) | 2.26 (0.44) | ND | ND | 0.84 (0.37) | 0.49 (0.22) | 0.29 (0.14) | 0.04 (0.02) |
| | SP3 | 5.33 (0.14) | 6.68 (1.33) | 1.57 (0.48) | ND | ND | 0.92 (0.18) | 0.50 (0.11) | 0.37 (0.12) | 0.03 (0.02) |
| | SP2 | 5.36 (0.19) | 8.48 (1.16) | 13.33 (10.01) | ND | ND | 0.80 (0.35) | 0.53 (0.22) | 0.42 (0.26) | 0.02 (0.02) |
| | SP1 | 5.62 (0.62) | 12.75 (6.13) | 8.85 (9.35) | ND | ND | 1.89 (0.90) | 0.91 (0.39) | 1.06 (1.26) | 0.05 (0.03) |
| | SP0 | 5.32 (0.05) | 8.33 (1.66) | 13.14 (5.03) | ND | ND | 1.12 (0.10) | 0.71 (0.06) | 0.37 (0.03) | 0.08 (0.07) |
| DOY 46 | SP4 | 5.38 (0.06) | 12.27 (3.21) | 6.26 (0.88) | 0.27 (0.36) | 0.92 (0.016) | 1.95 (0.85) | 1.12 (0.33) | 0.36 (0.04) | 0.13 (0.01) |
| | SP3 | 5.51 (0.07) | 17.25 (6.13) | 6.87 (1.57) | 0.45 (0.09) | 1.08 (0.057) | 3.10 (1.48) | 1.84 (0.66) | 0.88 (0.01) | 0.22 (0.14) |
| | SP2 | 5.27 (0.03) | 11.30 (4.84) | 11.14 (8.13) | 0.29 (0.31) | 1.00 (0.042) | 2.00 (1.13) | 1.15 (0.65) | 0.45 (0.11) | 0.13 (0.05) |
| | SP1 | 5.62 (0.30) | 44.43 (34.6) | 4.36 (1.90) | 0.27 (0.19) | 1.05 (0.12) | 9.74 (8.89) | 5.69 (4.52) | 0.95 (0.62) | 0.06 (0.05) |
| | SP0 | 5.53 (0.11) | 115.88 (48.7) | 18.98 (14.48) | 0.33 (0.12) | 1.15 (0.12) | 29.31 (12.91) | 15.19 (5.11) | 0.99 (0.22) | 0.04 (0.05) |

[a]Values are the average of triplicate samples from the top, middle, and basal snow (standard deviation in parentheses). "ND" means "not determined."

two groups of behavior: [Ca$^{2+}$, pH and DIC] and [Na$^+$ and Cl$^-$]. Neither of the biogeochemical parameters (Chlorophyll $a$, DOC, and NH$_4^+$) conformed with these two groups.

Figure 2a shows that there was markedly more Chlorophyll $a$ in the surface snows at the coastal sites SP0, SP1, and SP2 during the first two surveys (DOYs 24 and 35), when compared to their glacial counterparts at SP3 and SP4. However, no such differences were apparent by the time of the final survey (DOY 41), when the greatest Chlorophyll $a$ concentrations were in fact in the middle and lower parts of SP0 and SP2. The first
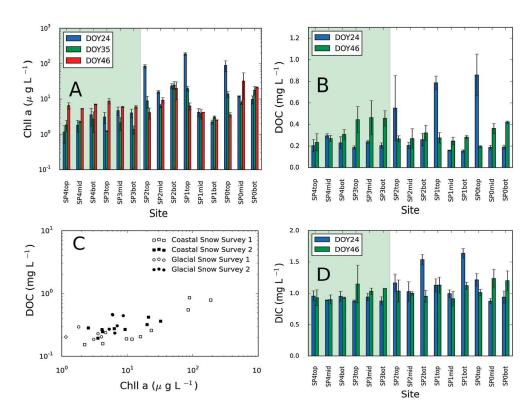


**Figure 2.** Biogeochemical conditions in the snowpits throughout the field work period. (a) Chlorophyll $a$ concentrations, (b) dissolved organic carbon concentrations (DOC), (c) the relationship between chlorophyll $a$ and DOC, and (d) dissolved inorganic carbon concentrations. The subscripts "top," mid, and "bot" refer to the position within the snowpit (see text for description). The error bars represent one standard deviation ($n = 3$). The green shading distinguishes the glacial snowpits (SP3 and SP4) from the coastal ones (SP0, SP1, and SP2).
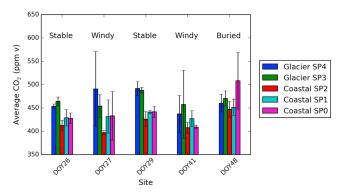
**Figure 3.** Depth-averaged $CO_2$ concentrations in snowpack air throughout the study. The error bars are standard deviations.

survey was also characterized by much more DOC in the surface snows at the coastal sites (Figure 2b), with these being the only samples exhibiting average values in excess of 0.5 mg $L^{-1}$. Samples were not collected for all parameters during the intermediate survey of DOY 35, and so DOC data are next available for the final survey on DOY 41, when they appear to be far more uniform across the sites (but greatest at SP3). The high values in the surface snow of the initial surveys caused a significant ($p < 0.01$) linear and positive correlation between Chlorophyll $a$ and DOC ($r^2 = 0.80$), which is also shown in Figure 2c. However, the end of summer survey produced no such relationship ($p = 0.23$, $r^2 = 0.11$). Alternatively, Figure 2c suggests that there was a strong, persistent correlation between Chlorophyll $a$ and DOC concentration in the coastal snows, regardless of the date of the survey ($p < 0.01$, $r^2 = 0.77$), while the relationship was much weaker in the glacial snows ($p = 0.03$, $r^2 = 0.39$).

The dissolved inorganic carbon (DIC) content of the snow is shown in Figure 2d and reveals that the greatest and most variable values were encountered in the coastal snowpacks during the first survey, especially at the surface and base. However, the DIC contents of all samples lay in the limited range of 0.8–1.6 mg $L^{-1}$. There was also some evidence of basal DIC enrichment at SP2 and SP1 during the first survey, when samples contained meltwater with fine inorganic debris. These higher DIC values were always associated with higher pH (>5.8), resulting in a significant ($p < 0.01$, $r^2 = 0.53$) positive linear correlation between pH and DIC during the first survey. However, once more, this correlation was not apparent during the final hydrochemical survey, when only one pH value greater than 5.8 was observed ($p = 0.06$, $r^2 = 0.12$). The DIC was also significantly correlated with $Ca^{2+}$ ($p < 0.01$, $r^2 = 0.76$ using both surveys), but none of the other solutes. Further, the correlation between $Ca^{2+}$ and pH was stronger ($r^2 = 0.84$, $p < 0.01$).

The EC levels described in Table 1 show that an increase in the total ionic solute content of the snow and liquid water mixtures occurred at the different sites toward the end of the field season. This increase was most marked at SP0 and was caused by solute derived from marine aerosol, resulting in very significant correlations between EC and both $Na^+$ and $Cl^-$ ($p < 0.01$; $r^2 = 0.96$ and 0.98, respectively). No significant patterns in the distribution of $NH_4^+$ were found. During the first snow survey, average concentrations shown in Table 1 were far-exceeded by concentrations in surface snows at the coastal sites SP0 and SP2 (i.e., 0.244 and 0.144 mg $L^{-1}$, respectively: data not shown). Similarly, the concentrations of $Na^+$ were greatest here (including also SP1), but there was no significant correlation between $Na^+$ and $NH_4^+$. Higher concentrations (i.e., > 0.1 mg $L^{-1}$ were also encountered at all snowpits in the final survey due to the fresh snowfall, producing the seasonal maximum average concentrations reported in Table 1.

Figure 3 shows the average snowpack air $CO_2$ concentrations, estimated from duplicate or triplicate samples taken from three depths at SP0, SP1, and SP2 and four depths at SP3 and SP4 (since these snowpits were in excess of 2 m deep). The depth-integrated average $CO_2$ concentrations were consistently greater at the glacial snowpits (SP4 and SP3) than at the coastal snowpits (SP2, SP1, and SP0), with the exception of DOY 48 at SP0. The differences in average $CO_2$ between data grouped together from the glacial versus the coastal snowpacks were statistically significant ($p \leq 0.01$) on DOYs 26, 27, and 29, but not DOYs 41 and 48. The latter results were collected during strong winds (DOY 41 only) and following fresh snowfall. Sampling conditions on DOY 27 were also very windy, and therefore, wind-pumping effects are thought to be linked to the high standard deviation of $CO_2$ concentrations apparent in Figure 3 for both DOYs 27 and 41. The greater standard deviations associated with depth-averaged $CO_2$ at SP4 and SP3 during DOY 27 were caused by high values just
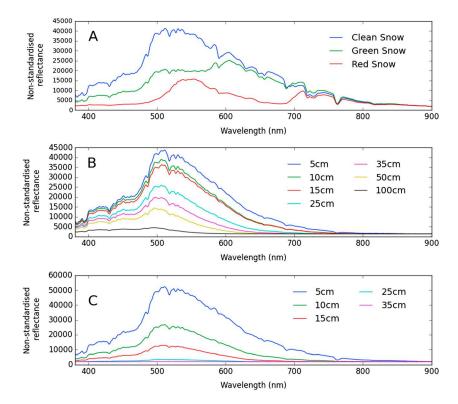
**Figure 4.** Examples of the spectroradiometric results of the different snow covers. (a) Reflectance spectra for the snow surface. (b and c) Vertical profiles of upwelling spectra at SP3 (DOY 30) and SP2 (DOY 41), respectively.

above an ice layer in the middle of the snowpack, where meltwater was observed during the first sampling survey (i.e., DOY 24). By contrast, the greater standard deviation associated with SP0 on the same day was associated with ponding at the base of the snowpack: an occurrence that was also associated with variable, high average $CO_2$ values at the same site on DOY 48 following its inundation by a meltwater stream. Therefore, no systematic variations in $CO_2$ with depth were observed, which is why we resort to showing just the average data here.

Average $CO_2$ levels in snowpack air were only depleted relative to the atmospheric boundary layer measurements at SP0, SP1, and SP2 during the first survey (DOY 26: data not shown). After this only occasional surface snow $CO_2$ levels were depleted relative to the atmosphere (e.g., at SP0 on DOY 41; SP2 on DOYs 27, 41, and 48; and SP4 on DOY 48: data not shown). However, the depletion was not statistically significant, and so only the difference between the coastal and the glacial snowpacks described above is considered to be a robust pattern.

### 3.2. Surface Spectra and Spectral Profiles of the Snowpacks

Examples of snow surface spectra are shown in Figure 4a, while Figures 4b and 4c show examples of the depth profiles of the upwelling spectra. The surface spectra shown in Figure 4a compare sites encountered during the transect study at SP2, including the most intensely discolored snow (showing both green and red pigmentation) and the visibly "cleanest" snow. The impact of green algae upon the reflectance spectra is clear between 600 and 700 nm, while the impact of the red colored algae is most obvious between 500 and 600 nm. In Figures 4b and 4c, clear evidence of the characteristic "blue-shift" in the spectra is also apparent with increasing depth, demonstrating how light in this part of the spectrum propagates furthest through snow and ice [*Warren*, 1982]. Figure 4c also demonstrates how fresh snow greatly influences the penetration and transmission of light within the various snowpacks. Therefore, while upwelling spectra were detectable as far down as 100 cm at SP3 on DOY 30 (Figure 4b), they were not detectable at 35 cm or below at SP2 on DOY 41 (Figure 4c), following the recent snowfall.

**Table 2.** Values of $K^{ext}$ Determined From the Upwelling Spectra at Various Wavelengths Through the Field Period

| Site/Date | 380 nm | 480 nm | 550 nm | 580 nm | 680 nm |
|---|---|---|---|---|---|
| SP0/DOY 29 | 5.36 | 9.133 | 10.06 | 9.917 | 8.45 |
| SP0/DOY 41 | 5.86 | 10.84 | 10.45 | 12.63 | 9.79 |
| SP1/DOY 29 | 7.58 | 12.44 | 8.40 | 10.87 | 11.57 |
| SP1/DOY 41 | 5.38 | 10.26 | 11.40 | 11.07 | 7.82 |
| SP2/DOY 29 | 4.72 | 7.23 | 6.201 | 7.731 | 8.52 |
| SP2/DOY 41 | 5.38 | 11.14 | 10.01 | 11.68 | 6.98 |
| SP3/DOY 29 | 1.08 | 1.57 | 3.25 | 3.52 | 5.02 |
| SP3/DOY 41 | 3.07 | 5.93 | 5.66 | 6.65 | 2.79 |
| SP4/DOY 29 | 0.93 | 1.48 | 1.00 | 4.18 | 4.18 |
| SP4/DOY 41 | 2.59 | 4.33 | 2.97 | 6.53 | 6.53 |
| Cells mL$^{-1}$ $r^2$, $p$[a] | 0.69, 0.003 | 0.52, 0.018 | 0.40, 0.050 | 0.38, 0.057 | 0.77, 0.001 |

[a]Also shown is the correlation between $K^{ext}$ and total (log. 10 transformed) autotrophic cell abundance.

The depth profiles of the upwelling spectra collected on DOYs 29 and 41 were used to estimate spectral extinction functions ($K^{ext}$) representative of the very different conditions at the beginning and end of the observation period. The functions took the usual form of

$$I_d = I_0 e^{-K^{ext}Z} \tag{1}$$

where $I$ is the measured irradiance at depth ("$I_d$") or at the surface ($I_0$) [see *Warren*, 1982]. Table 2 shows the estimates of $K^{ext}$ derived for specific wavelengths across the visible light spectrum (i.e., 380, 480, 580, and 680 nm) after fitting exponential regression models. The greatest coefficients indicate the least penetration through the snow, which was most often (but not always) observed at 580 nm. Greater extinction gradients were sometimes observed at both 480 and 680 nm, while 380 nm extinction coefficients were consistently the lowest, as is expected given the general optical properties of snow and its more effective transmission of light toward UV wavelengths [*Warren*, 1982]. The most notable feature of the light profiles, however, was that on both survey dates, the coefficients were always lowest for the glacial snowpacks SP3 and SP4 compared to their coastal counterparts, SP0–SP2. Therefore, solar transmission through the glacial snowpacks was most effective. For the second survey (DOY 41), greater extinction coefficients were observed at most sites on account of additional burial by a wet, fresh snow layer that had undergone less snow grain metamorphosis than the older underlying snow.

### 3.3. Snowpack Microbiology

The 16S rRNA illumina MiSeq data analysis at the phylum level showed that all pits were dominated (81–94%) by the Proteobacteria and Bacteroidetes. The next most abundant phyla were significantly lower in abundance and included Actinobacteria and Verrucomicrobia, with a minor contribution by Firmicutes, Acidobacteria, and Cyanobacteria. In the coastal snowpits, the dominance of the Proteobacteria and Bacteroidetes was marginally lower (81–85%) and a number of other phyla such as Planctomycetes were present (supporting information). Compared to the glacial snowpack, the coastal snowpack bacterial community therefore seemed more diverse, containing bacteria from various taxonomic groups including Alpha-, Beta-, Gamma-, and Delta-Proteobacteria; Sphingobacteria; Actinobacteria; Verrucomicrobiae: and Flavobacteria. Figure 5 shows that this difference is also easily discernable at the genus level: *Sphingomonas*, *Janthinobacterium*, and *Pedobacter* were the most abundant bacteria at SP3 and SP4 (glacial snows), while a far greater range was again apparent in coastal snows, with no clear dominance. As a result, the Inverse Simpson diversity index (1/D) of the glacial snowpacks was low (34 and 50 at SP4 and SP3, respectively) compared to the coastal snowpacks (between 119 and 530 at SP0, SP1, and SP2). At the species level (data not shown), the most common bacterium in the coastal snows was *Segetibacter aerophilus*, described from air samples as Gram-negative, strictly aerobic, nonmotile, and nonspore-forming rods capable of hydrolysing cellulose and starch [*Weon et al.*, 2010]. By contrast, there were 11 and 6 other more abundant species in the glacial snowpacks at SP3 and SP4, respectively. Here both pits showed the dominance of *Janthinobacterium lividum*, a species known for its general association with aquatic ecosystems, but also for being found in soils of the maritime Antarctic [*Shivaji et al.*, 1991] and for red or purple pigmentation
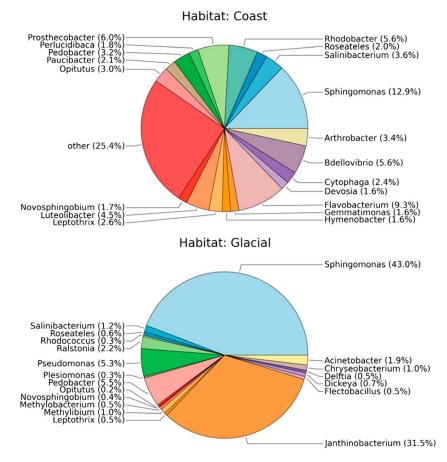
**Figure 5.** Taxonomic diversity at genus level for coastal (SP0, SP1, and SP2) and glacial (SP3 and SP4) snowpacks according to 16S rRNA results.

when grown at low temperatures [*Schloss et al.*, 2010]. The second-most abundant species at all sites except SP0 was *Sphingomonas echinoides*, a Gram-negative, yellow-pigmented aerobic bacterium that is known for being metabolically versatile [*Shin et al.*, 2012]. Other *Sphingomonas* spp. were also dominant at just SP3 and SP4. The importance of *Sphingomonas* spp. is also known from the study of bacterial diversity in local soils of the area [*Ganzert et al.*, 2011].

The taxonomy of the algae in snows from the study area has already been documented in detail by *Zidarova* [2008]. This work suggests that several species of Chlorophyta and diatoms may be expected in coastal snowpacks, including those known to occur in marine and soil ecosystems elsewhere in Antarctica. The Chlorophyta are known to be dominated by the snow algae, which we confirmed using epifluorescence microscopy (data not shown). In so doing, we observed that the autofluorescing community was clearly dominated by unicellular, nonflagellated red and green snow algae (assumed to be *Chlamydomonas* sp.) and included almost no filamentous cyanobacteria. The flow cytometry results also showed the presence of a clear population of large snow algal cells autofluorescing under the 488 nm laser in the FL3 channel. The concentration of these cells ranged from ~$1.1 \times 10^2$ cells mL$^{-1}$ in the case of snow from the middle of SP3 to $5.5 \times 10^5$ cells mL$^{-1}$ on the basal icing exposed at SP2. The corresponding Chlorophyll *a* concentration range was 1.23 to 5220 μg L$^{-1}$. As a result of the dominance of snow algae, a highly significant ($p < 0.01$, $r^2 = 0.992$) correlation between the total number of autofluorescing cells and the in vivo Chlorophyll *a* fluorescence signal was found, taking the form

$$\log_{10} \text{cells mL}^{-1} = 1.01\text{Chl}_a + 1.86 \tag{2}$$

The strong relationship shown in equation (2) therefore shows that the in vivo Chlorophyll *a* data presented in Table 1 and Figure 2 are a reliable indicator of the abundance of photosynthesising microorganisms in the snow. Inversion of this relationship implies a mean Chlorophyll *a* content of 12.8 pg Chl *a* cell$^{-1}$, which is reasonable given the abundance of large ($>1$ μm) snow algal cells observed using the microscope. The snow algal community in the present study therefore compares well with that described in earlier studies of both Alpine [*Thomas*, 1972; *Painter et al.*, 2001; *Takeuchi et al.*, 2006; *Lutz et al.*, 2014] and maritime Antarctic [*Fogg*, 1968] communities in terms of the abundance of cells causing strong discolouration of the snow surface.

## 4. Discussion

The results described above reveal an active snowpack microbial ecosystem which is notable for an autotrophic biomass dominated by the snow algae and a bacterial community dominated by Proteobacteria and Bacteroidetes. The microbial community therefore shares some characteristics with those observed in better known Alpine and Arctic snow ecosystems [e.g., *Amato et al.*, 2007; *Harding et al.*, 2011; *Hell et al.*, 2013; *Larose et al.*, 2010], as well as snows in the vicinity of Russian Antarctic research stations [*Lopatina et al.*, 2016]. For example, the importance of the Sphingobacteria, Flavobacteria, and Betaproteobacteria in coastal snows of the present study is similar to that described in snow lying upon soil in coastal Svalbard [*Larose et al.*, 2010]. These bacteria contribute to an important increase in the diversity of the bacterial community toward the coast. Here various other taxonomic groups were well represented, including Alpha-, Beta, Gamma-, and Delta-Proteobacteria; Sphingobacteria; Actinobacteria;Verrucomicrobiae; and Flavobacteria. *Hell et al.* [2013] also indicate the dominance of the Betaproteobacteria and report little diversity across a Svalbard glacier. The glacier snowpack microbial community also seemed largely composed of typical endogenous Antarctic snow inhabitants [*Lopatina et al.*, 2016], while the coastal snowpack contained taxa known from snow, ice, soils, and the ocean. We are confident that the sequences obtained represent genuine samples from the cryosphere due to their similarity to other snowpack and polar studies [e.g., *Pearce et al.*, 2016], the lack of such sequences in the controls, and their dissimilarity to those described from common reagent contaminants [e.g., *Salter et al.*, 2014]. Furthermore, the number of operational taxonomical units (OTUs) shared by the combined coastal snowpit bacterial communities (total 64,648) and the combined glacial snowpits (total 17,251) was very low (1528 or 2.3%), suggesting that the two different snowpack habitats harbored distinct bacterial communities. These differences suggest the greater diversity in the coastal snowpack communities most likely results from their closer proximity to marine and terrestrial ecosystems beyond the ice margin. The differences also suggest that there is clearly a need to account for this gradient when considering the response of the microbial communities of inland glacial snowpacks to climate warming.

### 4.1. Biogeochemical Properties of the Snowpacks

Establishing how the microbial community described above influences the physical and chemical conditions within the snow requires an appreciation of the changes that occurred between sampling. Specifically, this study captured the transition from midsummer to late summer, as brought about by the first significant fresh snowfall for some time. This fresh snow was then redistributed by wind and persisted until the end of our field work. These changes, along with the spatial heterogeneity of the surface snow algal blooms to start with, mean that changes in snow properties from one snow survey to the next must not be uncritically attributed to ecosystem processes. For example, surface snows in the shallower coastal snowpits (SP0–SP2) during the first two surveys (DOYs 24 and 35) were buried and became the midsnow later on DOY 41. This was not the case with the deeper ($>2$ m) glacial snowpits (SP3 and SP4), because the surface layer during the first surveys failed to reach the sampling point designated for "mid" snow. Therefore, the following discussion examines inter-relationships between key parameters, rather than simply their change from one survey to the next. In so doing we aim to demonstrate that the chemical and physical conditions within the snow habitat are, as with any ecosystem, clearly influenced by the presence of an active microbial community during the summer.

The strong, linear association between EC and both Na$^+$ and Cl$^-$ reveals that the total solute content (or ionic strength) of the snow was governed by marine aerosol. However, neither Cl$^-$ nor Na$^+$ were correlated with Ca$^{2+}$, suggesting the enhancement of solute within snowmelt by dust weathering. This was almost certainly possible under in situ conditions because the snowpacks lay entirely at the melting point during the first survey. For this reason, and because Ca$^{2+}$ concentrations sometimes exceeded those of Na$^+$ (Table 1), the weathering of dust and basal debris is likely an important contributor to the biogeochemical conditions of the

snowpack environment, resulting in the significant, linear correlations between $Ca^{2+}$ and both DIC and pH reported above. The linear regression model between all $Ca^{2+}$ and DIC data took the form

$$DIC = 0.25\left[Ca^{2+}\right] + 0.860 \tag{3}$$

The intercept value of 0.86 mg $L^{-1}$ is far in excess of the additional DIC that might be anticipated from the equilibration of the sample to the atmosphere during sample processing (i.e., $\leq$0.1 mg $L^{-1}$ according to thermodynamic data and the pH measurements), and so these data are notable for an additional, significant source of alkalinity not associated with the dust weathering. The presence of an additional DIC source is further supported by the fact that the $CO_2$ content of snowpack interstitial air was, more often than not, found to be in excess of atmospheric values (with the exception of the chlorophyll-rich surface snows discussed below). The most likely processes include microbial respiration and perhaps some contribution from the photolysis of organic carbon, although the latter seems unlikely given the much lower concentrations of DOC (Table 1). The residuals of the regression model in equation (3) were therefore examined, and statistically significant ($p < 0.05$), positive linear correlations found after logarithmic transformation of both the DOC concentration ($r^2 = 0.39$) and the Chlorophyll $a$ ($r^2 = 0.60$) data. No other biogeochemical parameters other than these were found to correlate significantly with residual DIC. The stronger correlation for Chlorophyll $a$ was surprising but implies that the autotrophic community was linked to the DIC content of the snow, with the most obvious explanations for the positive relationship being that net autotrophic respiration and/or the provision of labile DOC for an active heterotrophic community was occurring within the snow. Otherwise, we would have expected negative relationship due to $CO_2$ consumption during photosynthesis.

The significant correlation between Chlorophyll $a$ and DOC during the first snow survey and its subsequent demise by the time of the final snow survey suggest that autotrophic activity also increased the abundance of DOC within near-surface snow until the fresh snowfalls occurred. Further, the relationship ($p < 0.05$; $r^2 = 0.64$) between DOC and Chlorophyll $a$ during the second survey remained significant in just the coastal snowpacks (Figure 2c). However, at the glacial snowpits, although no statistically significant correlations between these parameters could be established, there was in fact a net direction of change in Chlorophyll $a$ and DOC from the first survey to the final one which was consistent with there being more primary production in the final survey samples (since both parameters increased: Table 1). This particular increase in biogeochemical parameters following the deposition of fresh snow onto the glacial snowpits was contrary to expectation but can be explained by the fact that the snow layer was largely fresh snow imported from elsewhere by strong winds. Therefore, it seems that the winds also imported microorganisms onto the glacial snowpit sites.

Other crucial nutrients for snowpack biological activity include $NH_4^+$, which is particularly important for autotrophic production [*Jones*, 1999] and bacterial ammonia oxidation [*Hell et al.*, 2013], but difficult to link to biological activity without examining the nutrient content of the cells themselves. *Hodson* [2006] and *Fujii et al.* [2010] used stable isotope measurements of $^{15}N$ abundance in snow, meltwater, and cells to show that $NH_4^+$ abundance and distribution in Antarctic snowfields may be greatly influenced by both assimilation and strong deposition gradients in the vicinity of marine fauna. For these reasons, and because $NH_4^+$ is readily produced by the evaporation of urea from guano (while other nutrients are not), the failure of $NH_4^+$ to correlate with other solutes in the present study was not surprising [see also *Hodson*, 2006].

## 4.2. Bio-Optical Properties of the Snowpacks

The biogeochemical conditions described above clearly indicate the influence of microbial populations in Livingston Island snowpacks, and so here we assess if the same can be said of the snow's optical properties. Specifically, we establish quantitative links between surface reflectance spectra and autotrophic cell density for the first time in Antarctica. Then, we examine the influence of the biomass on the extinction depth and spectral quality of light within the snowpack.

Pigments such as carotenoids and Chlorophyll $a$ that are associated with photosynthesising snow algae are well known to create absorption maxima in two narrow wavebands, around 450 nm and 680 nm, respectively [*Painter et al.*, 2001; *Cook et al.*, 2017]. Further strong absorption features associated with chlorophyll $a$ and $b$ occur near 430 nm, although here the masking effect of impurities such as dust and soot is also
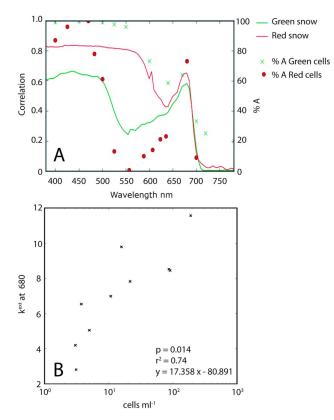
**Figure 6.** (a) The lines depict the coefficient of determination ($r^2$) for regression models at 5 nm increments between the log-transformed autotrophic cell abundance and standardized reflectance of the red and green snows at SP2. All correlations were negative. Data points show absorption spectra for individual red and green colored algal cells (after *Gorton et al.* [2001] and *Coltelli et al.* [2013], respectively). (b) Correlation between the autotrophic cell density and the vertical extinction coefficient of light at 680 nm wavelength.

significant [*Takeuchi et al.*, 2006]. However, Figure 6a shows that the effects of both pigments are clearly discernible at the snow surface, because the log-transformed autotrophic cell density observed in either red or green snows along the SP2 transect correlates best with standardized reflectance at the aforementioned wavelengths of light, where these pigments are known to be influential. In fact, Figure 6a shows that the reflectance correlations for both red and green snows bear a striking resemblance to the absorption spectra of single cells of red *Chlamydomonas nivalis* and other green algae (see *Gorton et al.* [2001] and *Coltelli et al.* [2013], respectively).

The correlations in Figure 6a are all highly significant ($p < 0.01$) below 570 nm in the case of red snows, and below 500 nm for green snow (although the latter are markedly weaker). These "plateaus" of uniform correlations lie across a broader part of the spectrum than can be explained by primary carotenoids and chlorophylls and therefore seem influenced by secondary carotenoids including astaxanthin, which have a maximum absorption

at 472 nm and an effect upon absorption to as low as 380 nm in the case of red colored algal cells according to *Gorton et al.* [2001]. That the effect of chlorophyll is most apparent in the green snows is hardly surprising, but it should be noted that astaxanthins are also present in green snow algae, albeit at much lower concentration [e.g., *Lutz et al.*, 2015]. Both red and green snow correlation spectra also show the well-known effect of chlorophyll pigments at 680 nm. Here correlations are also significant ($p < 0.05$) but are once more greatest for the red snow algae. The dramatic drop in correlation between biomass and reflectance above 680 nm can be explained by the lack of pigments absorbing at long visible light wavelengths and also the increasingly contrasting spectral reflectance between snow, firn, and ice at the red-end of the visible wave band (see *Zeng et al.* [1984, Figure 2] for comparison). This is especially significant because our study sites included dry snow, waterlogged snow, and thin snow layers over ice. Our data therefore illustrate the potential for extracting biological insight from snow spectral reflectance but also highlight the need for careful measurement and modeling of snow and/or ice physics.

Beneath the snow surface were significant differences in the vertical spectral extinction gradients ($K^{ext}$) of the glacial and coastal snowpacks (Table 2). These clearly suggested a greater number of impurities present in the coastal snows, because the extinction coefficients were greater across the broad range of wavelengths shown (i.e., from 380 to 680 nm). The impurities observed during sampling were snow algae, glacial moraine, volcanic ash, and organic detritus from wind-blown marine macroalgae and lichen. A contribution from soot was not discernible but can be expected on account of there being local sources associated with power generation. Surprisingly, little organic detritus was observed while digging and maintaining the pits. However,

reworked, wind-blown volcanic ash was obvious at all coastal sites, and filter papers revealed a dominant, minor supply of wind-blown gray moraine debris at SP1, SP3, and SP4.

Statistical analysis using regression modeling was used to establish whether the autotrophic community made an important contribution to the different extinction coefficients of the glacial and coastal snowpacks. We found that the number of autotrophic cells was the best predictor of the coefficients at 680 nm, indicating the influence of light absorption beneath the snow surface by Chlorophyll $a$ (see Table 2). Figure 6b shows this significant, positive and exponential relationship between the average number of autotrophs and $K^{ext}$ at 680 nm ($p < 0.01$; $r^2 = 0.77$). Far weaker correlations were found at 480, 550, and 580 nm (Table 2). Therefore, in contrast to the surface reflectance, the subsurface extinction coefficients revealed little control by carotenoid pigments. Since upwelling spectra were used, this is an intuitive outcome if the production of pigments like axastanthin is a surface phenomenon induced by high levels of irradiance and photoacclimation. Furthermore when the subsurface samples were viewed under the microscope, the community was dominated by spores of green colored algal cells that were aggregated to ~40 μm diameter. Therefore, we have demonstrated that both the surface and the subsurface optical properties of Antarctic snow are sensitive to the presence of the snow algal community. Since the optical properties of the snowpack influence its energy balance and melt rate, we advocate quantifying biological acceleration of Antarctic snowmelt as a research priority. This way we can better understand how biological growth in wet snow habitats influences the duration of snow cover and its role as a water and nutrient resource for downstream ecosystems.

## 5. Conclusions

Our work has shown that the biogeochemical and optical properties of Antarctic snow are directly influenced by the presence of a microbial community, especially near the coast. Autotrophic and heterotrophic microorganisms both appear to change the inorganic and organic carbon economies of the snowpack during summer. As a consequence, links between in situ rates of biological production within snow and the flux of nutrients carried by its meltwaters to downstream ecosystems require consideration if the full effects of warming in the Antarctic Peninsula are to be understood. We have also shown that melting may be directly influenced by the very presence of the microbial community, because the absorbance of solar radiation is enhanced by carotenoid pigments at the snow surface and by chlorophyll absorption beneath it.

Strong gradients in microbial biomass and community composition were encountered along short distances (<1 km) from the coastline during our study. Low-diversity, ultraoligotrophic ecosystems characterize inland snow covers on the glaciers, while order of magnitude increases in both species diversity and chlorophyll can be found at the coast. Therefore, while our results demonstrate that expansion of the melt zone into inland glacial snowpacks of the Antarctic Peninsula is likely to initiate microbial production and transformation of the snowpack nutrient resource found there, our work also shows that the uncritical upscaling of observations from snowpacks studied in close proximity to Antarctica's many coastal research stations should be avoided.

## References

Amato, P., R. Hennebelle, O. Magand, M. Sancelme, A. M. Delort, C. Barbante, C. Boutron, and C. Ferrari (2007), Bacterial characterization of the snow cover at Spitzberg, Svalbard, *FEMS Microbiol. Ecol.*, 59(2), 255–264.

Bañón, M., A. Justel, D. Velázquez, and A. Quesada (2013), Regional weather survey on Byers Peninsula, Livingston Island, South Shetland Islands, Antarctica, *Antarct. Sci.*, 25(02), 146–156.

Carpenter, E. J., S. Lin, and D. G. Capone (2000), Bacterial activity in South Pole snow, *Appl. Environ. Microbiol.*, 66, 4514–4517.

Coltelli, P., L. Barsanti, V. Evangelista, A. M. Frassanito, V. Passarelli, and P. Gualtieri (2013), Automatic and real time recognition of microalgae by means of pigment signature and shape, *Environ. Sci.: Processes Impacts*, 15(7), 1397–1410.

Cook, J. C., A. J. Hodson, A. Taggart, S. Mernild, and M. Tranter (2017), A predictive model for the spectral "bioalbedo" of snow, *J. Geophys. Res. Earth*, 122, 434–454, doi:10.1002/2016JF003932.

Dierssen, H. M., R. C. Smith, and M. Vernet (2002), Glacial meltwater dynamics in coastal waters west of the Antarctic peninsula, *Proc. Natl. Acad. Sci.*, 99(4), 1790–1795.

Edgar, R. C., B. J. Haas, J. C. Clemente, C. Quince, and R. Knight (2011), UCHIME improves sensitivity and speed of chimera detection, *Bioinformatics*, 27(16), 2194–2200, doi:10.1093/bioinformatics/btr381.

Edwards, H. G., L. F. De Oliveira, C. S. Cockell, J. C. Ellis-Evans, and D. D. Wynn-Williams (2004), Raman spectroscopy of senescing snow algae: Pigmentation changes in an Antarctic cold desert extremophile, *Int. J. Astrobiol.*, 3(02), 125–129.

Fogg, G. E. (1968), Observations on the snow algae of the South Orkney Is, *Phil. Trans. R. Soc. B*, 252, 279–287.

Fujii, M., Y. Takano, H. Kojima, T. Hoshino, R. Tanaka, and M. Fukui (2010), Microbial community structure, pigment composition, and nitrogen source of red snow in Antarctica, *Microb. Ecol.*, *59*(3), 466–475.

Ganzert, L., A. Lipski, H. W. Hubberten, and D. Wagner (2011), The impact of different soil parameters on the community structure of dominant bacteria from nine different soils located on Livingston Island, South Shetland Archipelago, Antarctica, *FEMS Microbiol. Ecol.*, *76*(3), 476–491.

Gorton, H. L., W. E. Williams, and T. C. Vogelmann (2001), The light environment and cellular optics of the snow alga *Chlamydomonas nivalis* (Bauer) Wille, *Photochem. Photobiol.*, *73*(6), 611–620.

Harding, T., A. D. Jungblut, C. Lovejoy, and W. F. Vincent (2011), Microbes in High Arctic snow and implications for the cold biosphere, *Appl. Environ. Microbiol.*, *77*(10), 3234–3243.

Hell, K., A. Edwards, J. Zarsky, S. M. Podmirseg, S. Girdwood, J. A. Pachebat, H. Insam, and B. Sattler (2013), The dynamic bacterial communities of a melting High Arctic glacier snowpack, *ISME J.*, *7*(9), 1814–1826.

Hodson, A. (2006), Biogeochemistry of snowmelt in an Antarctic glacial ecosystem, *Water Resour. Res.*, *42*, W11406, doi:10.1029/2005WR004311.

Jones, H. G. (1999), The ecology of snow-covered systems: a brief overview of nutrient cycling and life in the cold, *Hydrol. Processes*, *13*(14–15), 2135–2147.

Klindworth, A., E. Pruesse, T. Schweer, J. Peplies, C. Quast, M. Horn, and F. O. Glöckner (2013), Evaluation of general 16S ribosomal RNA gene PCR primers for classical and next-generation sequencing-based diversity studies, *Nucleic Acids Res.*, *41*(1), 1–11, doi:10.1093/nar/gks808.

Kohshima, S., Y. Yoshimura, K. Seko, and T. Ohata (1994), Albedo reduction by biotic impurities on a perennial snow patch in the Japan alps, *IAHS Publ.-Ser. Proc. Rep.-Intern. Assoc. Hydrol. Sci.*, *223*, 323–330.

Larose, C., S. Berger, C. Ferrari, E. Navarro, A. Dommergue, D. Schneider, and T. M. Vogel (2010), Microbial sequences retrieved from environmental samples from seasonal Arctic snow and meltwater from Svalbard, Norway, *Extremophiles*, *14*(2), 205–212.

Liston, G. E., and J.-G. Winther (2005), Antarctic surface and subsurface snow and ice melt fluxes, *J. Climatol.*, *18*, 1469–1481.

Lopatina, A., S. Medvedeva, S. Shmakov, M. D. Logacheva, V. Krylenkov, and K. Severinov (2016), Metagenomic analysis of bacterial communities of Antarctic surface snow, *Front. Microbiol.*, *7*, doi:10.3389/fmicb.2016.00398.

López-Martínez, J., E. Serrano, T. Schmid, S. Mink, and C. Linés (2012), Periglacial processes and landforms in the South Shetland Islands (northern Antarctic Peninsula region), *Geomorphology*, *155*, 62–79.

Lutz, S., A. M. Anesio, S. E. J. Villar, and L. G. Benning (2014), Variations of algal communities cause darkening of a Greenland glacier, *FEMS Microbiol. Ecol.*, *89*, 402–414.

Lutz, S., A. M. Anesio, K. Field, and L. G. Benning (2015), Integrated 'omics', targeted metabolite and single-cell analyses of Arctic snow algae functionality and adaptability, *Front. Microbiol.*, *6*, doi:10.3389/fmicb.2015.01323.

Marker, A. F. H., and S. Jinks (1982), Spectrophotometric analysis of chlorophyll a and phaeopigments in acetone, ethanol and methanol, *Ergebnisse der Limnol.*, *16*, 3–17.

Painter, T. H., B. Duval, W. H. Thomas, M. Mendez, S. Heintzelman, and J. Dozier (2001), Detection and quantification of snow algae with an airborne imaging spectrometer, *Appl. Environ. Microbiol.*, *67*(11), 5267–5272.

Pearce, D. A., I. Magiopoulos, M. Mowlem, M. Tranter, G. Holt, J. Woodward, and M. J. Siegert (2016), Microbiology: Lessons from a first attempt at Lake Ellsworth, *Phil. Trans. R. Soc. A*, *374*, 20140291, doi:10.1098/rsta.2014.0291.

Quast, C., E. Pruesse, P. Yilmaz, J. Gerken, T. Schweer, P. Yarza, J. Peplies, and F. O. Glöckner (2013), The SILVA ribosomal RNA gene database project: Improved data processing and web-based tools, *Nucleic Acids Res.*, *41*(D1), 590–596, doi:10.1093/nar/gks1219.

Salter, S. J., M. J. Cox, E. M. Turek, S. T. Calus, W. O. Cookson, M. F. Moffatt, P. Turner, J. Parkhill, N. J. Loman, and A. W. Walker (2014), Reagent and laboratory contamination can critically impact sequence-based microbiome analyses, *BMC Biol.*, *12*(87), doi:10.1186/s12915-014-0087-z.

Schloss, P. D., et al. (2009), Introducing mothur: Open-source, platform-independent, community-supported software for describing and comparing microbial communities, *Appl. Environ. Microbiol.*, *75*(23), 7537–7541.

Schloss, P. D., H. K. Allen, A. K. Klimowicz, C. Mlot, J. A. Gross, S. Savengsuksa, J. McEllin, J. Clardy, R. W. Ruess, and J. Handelsman (2010), Psychrotrophic strain of Janthinobacterium lividum from a cold Alaskan soil produces prodigiosin, *DNA Cell Biol.*, *29*(9), 533–541.

Shin, S. C., S. J. Kim, D. H. Ahn, J. K. Lee, and H. Park (2012), Draft genome sequence of Sphingomonas echinoides ATCC 14820, *J. Bacteriol.*, *194*(7), 1843–1843.

Shivaji, S., M. K. Ray, G. S. Kumar, G. S. N. Reddy, L. Saisree, and D. D. Wynn-Williams (1991), Identification of Janthinobacterium lividum from the soils of the islands of Scotia Ridge and from Antarctic peninsula, *Polar Biol.*, *11*(4), 267–271.

Takeuchi, N., R. Dial, S. Kohshima, T. Segawa, and J. Uetake (2006), Spatial distribution and abundance of red snow algae on the Harding Icefield, Alaska derived from a satellite image, *Geophys. Res. Lett.*, *33*, L21502, doi:10.1029/2006GL027819.

Thomas, W. H. (1972), Observations on snow algae in California, 2, *J. Phycol.*, *8*(1), 1–9.

Thomas, W. H., and B. Duval (1995), Sierra-Nevada, California, USA, snow algae—Snow albedo changes, algal bacterial interrelationships, and ultraviolet-radiation effects, *Arct. Alp. Res.*, *27*, 389–399.

Vaughan, D. G. (2006), Recent trends in melting conditions on the Antarctic Peninsula and their implications for ice-sheet mass balance, *Arct. Antarct. Alp. Res.*, *38*, 147–152.

Warren, S. G. (1982), Optical properties of snow, *Rev. Geophys.*, *20*, 67–89, doi:10.1029/RG020i001p00067.

Weon, H. Y., S. W. Kwon, J. A. Son, S. J. Kim, Y. S. Kim, B. Y. Kim, and J. O. Ka (2010), Adhaeribacter aerophilus sp. nov., Adhaeribacter aerolatus sp. nov. and Segetibacter aerophilus sp. nov., isolated from air samples, *Int. J. Syst. Evol. Microbiol.*, *60*(10), 2424–2429.

Zeng, Q., M. Cao, X. Feng, F. Liang, X. Chen, and W. Sheng (1984), A study of spectral reflection characteristics for snow, ice and water in the north of China, *Hydrol. Appl. Remote Sens. Remote Data Trans.*, *145*, 451–462.

Zidarova, R. (2008), Algae from Livingston Island (S Shetland Islands): A checklist, *Phytol. Balcanica*, *14*, 19–35.